Motor Parameter-Free Predictive Current Control of Synchronous Motors by Recursive Least-Square Self-Commissioning Model

Motor Parameter-free Predictive Current Control of Synchronous Motors by Recursive Least Square Self-Commissioning Model

F. Tinazzi, *Member*, *IEEE*, P. G. Carlet, S. Bolognani, *Fellow Member*, *IEEE*, and M. Zigliotto, *Senior Member*, *IEEE*

***Abstract*—This paper deals with a finite-set model predictive current control in synchronous motor drives. The peculiarity is that it does not require the knowledge of any motor parameter. The inherent advantage of this method is that the control is self-adapting to any synchronous motor, thus easing the matching between motor and inverter coming from different manufacturers. Overcoming the flaws of the existing look-up table based parameter-free techniques, the paper elaborates the past current measurements by a recursive least square algorithm to estimate the future behaviour of the current in response to a finite-set of voltage vectors. The paper goes through the mathematical basis of the algorithm till a complete set of experiments that prove the feasibility and the advantages of the proposed technique.**

***Index Terms*—Model predictive control (MPC), parameter-free, recursive least square (RLS), synchronous motor, PMSM, IPM.**

I. Introduction

Model Predictive Control (MPC) represents a promising architecture in electric drives applications, because of high dynamic performances, relatively easy tuning and possibility of including constrains in the problem resolution [1], [2]. The higher computational cost with the respect to PI controllers have represented a critical disadvantage in real-time implementation, as electric drives. However, nowadays fast processors and new platforms hardware, e.g. DSP-FPGA solutions, are available, thus interest in MPC is further increased [1].

The MPC principle consists into predicting the system dynamic in a future time window and choosing the optimal control input on the basis of a functional cost. Various aspects concerning the optimal functioning of the motor drive can be considered, such as the reduction of common-mode voltage [3], field-weakening operations of interior permanent magnet motors [4], thermal stress of the inverter [5] or even special machines, such as dual three-phase motors [6]. Furthermore, an integral action can be included in MPC algorithms such as in [7], [8]. There are mainly two approaches to MPC problem formulation based on the input voltage to be considered. The first group considers a continuous control signal to be generated by means of a modulator. The second group exploits the discrete nature of inverters, thus reducing the number of possible control actions. This method is named finite-set MPC and it is considered in this work. A detailed discussion about the differences between the two approaches is reported in [1]. The finite-set policy has been largely investigated in both electric motor and power converter control. A relatively low computational burden is required when inverters have a low number of levels, e.g. two levels, and short prediction horizons are chosen.

In general, systems dynamics prediction require an internal model of the specific process. Focusing on synchronous motors, the voltage balance equations in the dq reference frame is generally adopted. The electric parameters of the motor must be known, e.g. stator resistance, apparent and differential inductances. However, considering for instance multi-purpose drives applications, motor parameters are not always available. This could be the case of motor and inverter produced by different companies. In this case, only nominal motor data are given, which are affected at least by production variability. It is worth noticing also that both stator resistance and inductance parameters depends on the operating conditions of the motor, i.e. temperature and magnetic saturation, respectively [9], [10].

The most common countermeasures rely on ad-hoc self-commissioning procedures which are carried out during motor installation or production. Scientific literature is vast in this field [11]–[13]. Another practical approach is to combine already known information with online estimation of the parameters. For instance, when nominal parameters are provided, different observers can be implemented to adapt parameters value in the whole operating region [14]–[17].

An interesting solution is reported in [18], where the inductance variation is nested in the MPC formulation, providing also an integral-like action on the current tracking. The drawback is that the current prediction error is ascribed to the inductance variation, without considering the resistance and permanent magnet flux linkages variations and with the inverter non idealities perfectly compensated.

A new paradigm in the predictive control research is to

Manuscript received May 29, 2019; revised July 30, 2019 and October 25, 2019; accepted November 22, 2019. This work was supported in part by the Project SID 2017 -BIRD175428, financed by the University of Padova.

F. Tinazzi and M. Zigliotto are with Dept. of Management and Engineering, University of Padova, Italy. (e-mail: {fabio.tinazzi, mauro.zigliotto}@unipd.it

S. Bolognani and P. G. Carlet are with the Department of Industrial Engineering, University of Padova, Padova 35122, Italy (silverio.bolognani@unipd.it, paologherardo.carlet@phd.unipd.it).

completely skip the motor parameters knowledge, resorting to a motor parameter-free approach to carry out the current prediction. This eases the matching between motor and inverter, useful in case of different manufacturers.

Parameter-free predictive current control is generally based on a finite-set voltage vectors. The first work in this field, [19], adopted look-up tables (LUTs) for storing the current variations related to each of the eight base voltage vectors. This information is used to predict the best voltage vector to be applied, according to a predetermined cost function. The method suffered of a *stagnation* problem, due to the fact that if a voltage vector is not applied for many consecutive time steps, the stored information regarding the related current variation becomes obsolete. Two methods have been proposed to partially solve the stagnation problem so far. A *direct* method, proposed in [20], consists in modifying the cost function to force arbitrarily the application of voltage vectors not applied for long time. Of course, the arbitrary modification of the cost function acts as a disturbance in pursuing the desired control target. Conversely, *indirect* method have been proposed in [21], [22] to avoid the modification of the cost function. The LUTs update is carried out by reconstructing the current variations by specific mathematical relationships among the inverter voltage vectors at the cost of an increased complexity of the control algorithm. The information obsolescence is emphasised by both the fast changing of the operating point and the motor speed.

The research described in this paper is still around a parameter-free finite-set MPC current controller, but the problem of stagnation is definitely overcome by a new approach to the current prediction. To this aim, the model for the current prediction is derived by a particular recasting of the standard dq voltage equation.

The proposed method requires four coefficients, that are estimated by taking advantage of the information nested in the past measured current variations induced by known voltage vectors. A Recursive Least Squares (RLS) algorithm carries out the task of adapting the model parameters runtime. The sensitivity of the current prediction on both the operating point and the speed is greatly reduced.

The paper is organised as follows. Sect. II describes the recasting of the standard motor dq voltage balance equations. Sect. II-A reports the application of the RLS algorithm with some design hints. Sect. III presents the complete motor parameter-free finite-set MPC, whereas Sect. IV details the experimental tests and compares them with those of other MPC algorithms. Conclusions are reported in Sect. V.

II. Theory of operation

A finite-set MPC current controller requires a model of the current behaviour to predict synchronous motors dynamic. In order to design a finite-set MPC scheme that does not need any motor information, all the parameters used in the prediction phase have to be on-line identified.

To ease the mathematical representation, only the d-axis equation of a synchronous motor is considered. Equation of the q-axis dynamic is identical and lead to similar results, as summarised at the end of this Section.

$$\begin{aligned} u_d &= Ri_d + \frac{d\lambda_d(i_d,i_q)}{dt} - \omega_{\mathrm{e}}\lambda_q(i_d,i_q) \\ &= Ri_d + l_d(i_d,i_q)\frac{di_d}{dt} - \omega_{\mathrm{e}}\lambda_q(i_d,i_q) \end{aligned} \tag{1}$$

where u_d and i_d are the d-axis voltage and current, respectively, i_q is the q-axis current, R is the stator resistance, $\lambda_d(i_d,i_q)$ and $\lambda_q(i_d,i_q)$ are the d- and q-axis flux linkages, respectively, $l_d(i_d,i_q) \triangleq \partial\lambda_d(i_d,i_q)/\partial i_d$ is the differential d-axis inductance and ω_{e} is the motor electric speed obtained multiplying the mechanical speed by the pole pairs number. The magnetic cross-coupling between d and q axes is neglected.

The motor current dynamic is commonly described on the basis of the discretized voltage balance in the dq synchronous reference frame. In turn, the discretisation of the current derivative yield $di_d/dt \approx \Delta i_d(k)/T_c = (i_d(k) - i_d(k-1))/T_c$, where T_c is the control sampling time. The last of (1) can be discretised at time kT_c as follows:

$$\frac{\Delta i_d(k)}{T_c} = -\frac{Ri_d(k) - \lambda_q(k)\omega_{\mathrm{e}}(k)}{l_d(k)} + \frac{u_d(k)}{l_d(k)} \tag{2}$$

where $\lambda_q(k) = \lambda_q(i_d(k), i_q(k))$ and $l_d(k) = l_d(i_d(k), i_q(k))$. Equivalent equations can be written also for the q-axis. To ease the mathematical representation the time step dependence (k) is omitted in the rest of the paper, whereas preference is given to highlight the dependence of the motor parameters and quantities on the dq currents.

The d-axis current increment (2) can be represented as the sum of two terms. The first one is obtained by applying a null voltage to the system:

$$\delta i_d^0(i_d,i_q,\omega_{\mathrm{e}}) = -\frac{RT_c}{l_d(i_d,i_q)}i_d + T_c\omega_{\mathrm{e}}\frac{\lambda_q(i_d,i_q)}{l_d(i_d,i_q)} \tag{3}$$

The second term is obtained by the application of one of the other six (active) voltage vectors of the inverter:

$$\delta i_d^f(i_d,i_q,\vartheta_{\mathrm{e}},v) = \frac{T_c}{l_d(i_d,i_q)}\frac{2U_{dc}}{3}\cos\left((v-1)\frac{\pi}{3} - \vartheta_{\mathrm{e}}\right) \tag{4}$$

where ϑ_{e} is the electric angle, U_{dc} is the DC-bus voltage and $v \in \mathcal{U} \triangleq [1\dots6]$ is the index of the applied voltage vector. The overall current variation in (2) can be expressed as:

$$\Delta i_d(k) = \delta i_d^0(i_d,i_q,\omega_{\mathrm{e}}) + \delta i_d^f(i_d,i_q,\vartheta_{\mathrm{e}},v) \tag{5}$$

By putting

$$p_{1,d} \triangleq \delta i_d^0(i_d,i_q,\omega_{\mathrm{e}}); \qquad p_{2,d} \triangleq \frac{T_c}{l_d(i_d,i_q)}\frac{2U_{dc}}{3} \tag{6}$$

the d-axis current variation (5) can be rearranged as follows:

$$\Delta i_d^v = \left[1,\, \cos\left((v-1)\frac{\pi}{3} - \vartheta_{\mathrm{e}}\right)\right]\left[p_{1,d},\, p_{2,d}\right]^{\mathrm{T}} = \boldsymbol{\phi}^v\ \mathbf{p}_d \tag{7}$$

The vector of coefficients $\mathbf{p}_d$ is defined as $[p_{1,d},\ p_{2,d}]^T$. It is worth pointing out that the regressors $\boldsymbol{\phi}^v$ change with the considered voltage vector v. Finally, the current variations can be calculated by means of (7) without prior knowledge of the motor parameters, provided that the elements of $\mathbf{p}_d$ are known.

Similarly, the q-axis current variations are calculated as:

$$\delta i_q^0(i_d, i_q, \omega_e) = -\frac{RT_c}{l_q(i_d, i_q)} i_q - T_c \omega_e \frac{\lambda_d(i_d, i_q)}{l_q(i_d, i_q)} \quad (8)$$

$$\delta i_q^f(i_d, i_q, \vartheta_e, v) = \frac{T_c}{l_q(i_d, i_q)} \frac{2U_{dc}}{3} \sin\left((v-1)\frac{\pi}{3} - \vartheta_e\right) \quad (9)$$

where $l_q(i_d, i_q) \triangleq \partial\lambda_q(i_d, i_q)/\partial i_q$ is the q-axis differential inductance and $\lambda_d(i_d, i_q)$ is the d-axis flux linkage. An identical approach is used to obtain the $\mathbf{p}_q$ coefficients that describe the q-axis current variations, i.e. $\Delta i_q^v = \delta i_q^0 + \delta i_q^f$, leading to:

$$\Delta i_q^v = \left[1,\, \sin\left((v-1)\frac{\pi}{3} - \vartheta_e\right)\right] \left[p_{1,q},\, p_{2,q}\right]^{\mathrm{T}} = \boldsymbol{\phi}^v\, \mathbf{p}_q \quad (10)$$

A. The Recursive Least Square Estimator

The elements of $\mathbf{p}_d$ and $\mathbf{p}_q$ have to be estimated online. For the sake of brevity, only $\mathbf{p}_d$ estimation is discussed in this paper, bearing in mind that $\mathbf{p}_q$ can be estimated using the same approach. It is worth highlighting that $\mathbf{p}_d$ is time variant. In particular, $p_{1,d}$ depends both on the operating speed and magnetic iron saturation, see (3), whereas $p_{2,d}$ depends only on magnetic iron saturation, see (4).

The RLS technique is one of the most widespread method for estimating parameters during normal operations of a process [23]. It is particularly suited for applications that require adaptability to different working conditions. For these reasons it was adopted for estimating $p_{1,d}$ and $p_{2,d}$ that are the working point dependent coefficients.

The standard algorithm consists of a set of equations that can be solved recursively:

$$\begin{aligned} \mathbf{G}(k) &= \mathbf{Q}(k-1)\mathbf{\Phi}^T(k)(\mathbf{\Phi}\mathbf{Q}(k-1)\mathbf{\Phi}^T(k) + f\mathbf{I})^{-1} \\ \widehat{\mathbf{p}}_d(k) &= \widehat{\mathbf{p}}_d(k-1) + \mathbf{G}(k)\,(\mathbf{y}(k) - \mathbf{\Phi}(k)\widehat{\mathbf{p}}_d(k-1)) \\ \mathbf{Q}(k) &= \frac{1}{f}(\mathbf{Q}(k-1) - \mathbf{G}(k)\mathbf{\Phi}(k)\mathbf{Q}(k-1)) \end{aligned} \quad (11)$$

The estimated parameter vector $\widehat{\mathbf{p}}_d(k)$ is computed recursively minimising the error between measured current variation stored in $\mathbf{y}$ and the model presented in (7). The same set of equations apply for the estimation of $\widehat{\mathbf{p}}_q(k)$, too. Matrix $\mathbf{G}(k)$ is the gain matrix and it weights the error between measurements and estimations in the coefficients vector updates. The regressors matrix $\mathbf{\Phi}(k) = [\boldsymbol{\phi}^v(k),\, \boldsymbol{\phi}^v(k-1),\, \ldots]^{\mathrm{T}}$ includes all the regressors vectors $\boldsymbol{\phi}^v$ related to the measured current variations involved in the $\widehat{\mathbf{p}}_d(k)$ estimation, i.e. the ones related to the measurements $\mathbf{y}(k) = [\Delta i_d^v(k),\, \Delta i_d^v(k-1),\, \ldots]^{\mathrm{T}}$. Finally, $\mathbf{Q}(k)$ is the estimation error covariance matrix. A forgetting factor f is also introduced in (11) to properly weight the old data in the estimation, and its value determination is discussed in Sect. IV-B.

Being two the number of elements in $\widehat{\mathbf{p}}_d(k)$, the vector $\mathbf{y}(k)$ should have at least size 2×1 (and $\mathbf{\Phi}$(k), accordingly, at least size 2×2). In other words, at least two current variations measurements are requested in (11).

There are several possibility to select the measurements $\mathbf{y}(k)$. A first solution consists of using the last two measured current variations, i.e. $\Delta i_d^v(k-1)$ and $\Delta i_d^v(k)$, independently from the voltages applied in the considered control periods. A situation that may occur is when the same voltage vector is applied in two (or more) consecutive time steps. The RLS might turn out to be an ill-conditioned problem, and unexpected results could be obtained. In turn, it is difficult to estimate two different parameters from very similar measurements.

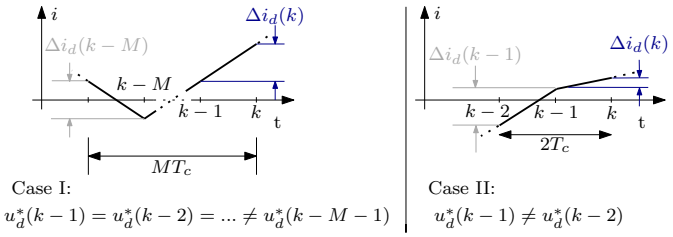

Fig. 1. Different cases evaluation for the regressors vector ϕ calculation.

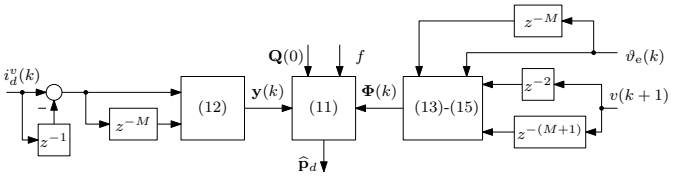

Fig. 2. Implementation of the RLS algorithm for estimating $\widehat{\mathbf{p}}_d$. The same applies for $\widehat{\mathbf{p}}_q$ estimation.

Another solution is to exploit the last measured current variation $\Delta i_d^v(k)$, whereas the second variation $\Delta i_d^v(k-M)$ is measured M time instants before. Therefore, the vector of measurements in (11) is defined as:

$$\mathbf{y}(k) = [\Delta i_d^v(k),\, \Delta i_d^v(k-M)] \quad (12)$$

The value of M is equal to the number of time steps from the application of a voltage vector different from the one applied at the beginning of $(k-1)$. This corresponds to Case I of Fig. 1. For instance, the same voltage vector can be applied for M consecutive time steps. Thus, the previous voltage vector different respect to the one applied at $(k-1)$ can be found at $(k-M-1)$.

Adopting the second strategy, the RLS algorithm works within a variable length time window. The minimum length is equal to two, as shown in the Case II of Fig. 1. It happens when two different voltages are applied in two consecutive time steps. The last applied voltage vector gives:

$$\boldsymbol{\phi}^v(k) = \left[1,\, \cos\left((v(k-1)-1)\frac{\pi}{3} - \vartheta_e(k)\right)\right] \quad (13)$$

whereas the last different voltage vector $v(k-M-1)$ returns:

$$\boldsymbol{\phi}^v(k-M) = \left[1,\, \cos\left((v(k-M-1)-1)\frac{\pi}{3} - \vartheta_e(k-M)\right)\right] \quad (14)$$

so that the regressors vector actually used in (11) is:

$$\mathbf{\Phi}(k) = [\phi^v(k),\, \phi^v(k-M)] \quad (15)$$

The outlined algorithm is summarised in the block schematic of Fig. 2.

In steady state conditions, the estimated $\widehat{\mathbf{p}}_d(k)$ values are not influenced by the time window length. The free response (3) and the amplitude of(4) are constant when i_d, i_q and ω_e are constant.

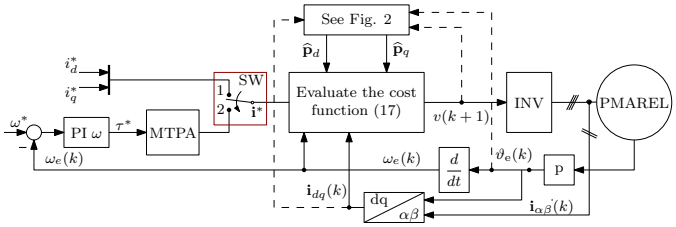

Fig. 3. Scheme of the proposed predictive current control algorithm. The state of the switch SW determines either current ($SW = 1$) or speed ($SW = 2$) control mode.

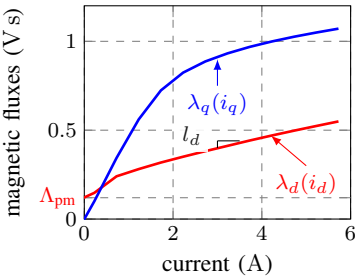

Fig. 4. PMAREL flux current characteristic.

The estimation of $\widehat{\mathbf{p}}_d(k)$ is critical during transients, in particular when Case I of Fig.1 occurs. The old measurement $\Delta i_d(k-M)$ carries information of the system in a previous operating point. Therefore, an error on the coefficients $\widehat{\mathbf{p}}_d$ estimation occurs. It is hard to draw a theoretical analysis on this side effect, since many different cases can happen. Therefore, this aspect is discussed by means of simulations and experiments in Sec. IV. Furthermore, it is expected that the choice of the forgetting factor f affects the transient behaviour of the RLS algorithm.

III. Motor Parameter-Free Predictive Control Algorithm

The aim of this section is to show how the current predictions can be calculated without the knowledge of the motor parameters. The d-axis current variation can be obtained by (7) using $\widehat{\mathbf{p}}_d$, which can be calculated as in (11), instead of $\mathbf{p}_d$. The q-axis current variation can be obtained using the coefficients $\widehat{\mathbf{p}}_q$ in (10). The optimal voltage vector $\mathbf{u}$ to be applied at time $k+1$ is obtained by minimising the error

$$\mathbf{e}(k) = \mathbf{i}^* - \widehat{\mathbf{i}}(k+2) \tag{16}$$

which corresponds to the following minimisation problem

$$v(k+1) = \min_{v \in \mathcal{U}} \mathbf{e}^T(k) \cdot \mathbf{e}(k) \tag{17}$$

where $\mathbf{i}^*$ is the vector current references at time step $(k+1)$ and $\widehat{\mathbf{i}}(k+2)$ is the vector of the current estimates. In this work, the prediction horizon is set at 2 to compensate for the computation delay in the digital implementation of the finite-set model predictive control algorithm.

The first step to solve the problem in (17) is computing the current estimate at time $(k+1)$. The voltage vector $\mathbf{u}(k)$ is known and $\widehat{\mathbf{i}}(k+1)$ can be calculated applying (7) just once for each of the dq currents.

The second step is to calculate the current estimates at time $(k+2)$. Since the voltage vector has not been decided yet, it is necessary to evaluate the current prediction for all the voltage vectors in the set $\mathcal{U}$. The current estimates $\widehat{\mathbf{i}}(k+2)$ can be calculated by applying (7) for each of the voltage vectors in $\mathcal{U}$. The solution that satisfies the problem in (17) is thus selected and the voltage vector reference $\mathbf{u}(k+1)$ is obtained accordingly. In other words, the output of the problem (17) is the index $v(k+1)$, i.e. the index of the voltage vector to be applied at time instant $(k+1)$.

TABLE I
Parameters of the Motor Under Test

Motor Data	Symbol	Values
Pole pairs	p	2
Phase resistance	R	$4.6\,\Omega$
d-axis inductance (unsaturated)	L_d	$0.160\,\text{H}$
q-axis inductance (unsaturated)	L_q	$0.450\,\text{H}$
Permanent Magnet flux-linkage	Λ_{pm}	$0.12\,\text{V s}$
Nominal current	I_N	$6\,\text{A}$
Nominal speed	Ω_N	$700\,\text{rpm}$

It is worth noting that (7) requires the electrical position ϑ_e. Since the voltage reference is actually applied at time $(k+1)$, it is correct to use the electrical position at time $(k+1)$. However, $\vartheta_e(k+1)$ is unknown. It is possible to estimate its value by imposing that the speed variation during one time step T_c is negligible. Therefore, the position $\vartheta_e(k+1)$ can be estimated assuming a constant speed within the prediction horizon, i.e. using a linear extrapolation:

$$\widehat{\vartheta}_e(k+1) = \vartheta_e(k) + \omega_e(k) T_c \tag{18}$$

The scheme of the proposed motor parameter-free predictive current control is summarised in Fig. 3 . The updating logic for the value of M is quite simple: the condition $v(k-1) \neq v(k-M)$ must always be satisfied and M must be as low as possible. It is straightforward that the minimum value of M is 2.

IV. Experimental Results and Discussion

The proposed control scheme has been implemented by means of a dSPACE MicroLabBox board. The rig layout consists of two motors mechanically coupled. The motor under test is a permanent magnet assisted reluctance (PMAREL) synchronous motor. A second motor is mechanically coupled to the PMAREL motor and acts as a programmable load. Motor parameters and both the measured d-q flux-current curves are provided in TABLE I and Fig. 4, respectively. All the tests were carried out with a constant DC bus of $300\,\text{V}$.

The currents responses in the following results are reported in $p.u.$. Where not specified, the normalisation quantities correspond to the maximum torque-per-ampere (MTPA) operating point at nominal current, i.e. $(i_d,\, i_q) = [-4.42\,\text{A},\, 4.05\,\text{A}]$. The speed results are also normalised with respect to the nominal speed value.

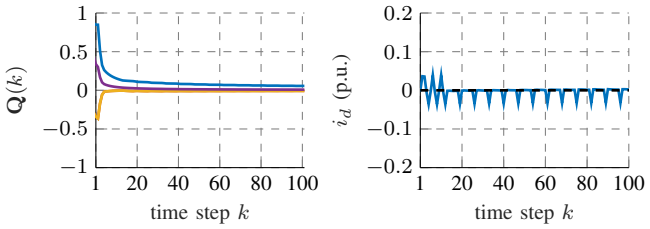

Fig. 5. d-axis covariance $\mathbf{Q}$ and current at the startup.

A. Initialisation of the RLS algorithm

At the startup, the RLS algorithm in (11) is initialised with a null estimated coefficient vector, i.e. $\widehat{\mathbf{p}}_d(0) = [0; 0]$, and an identity covariance matrix $\mathbf{Q}(0)$. This is a common solution when *a priori* information are not available [23].

Fig. 5 (left) reports the evolution of the covariance matrix $\mathbf{Q}$ elements at the startup. The random initialisation of the covariance matrix does not influence significantly the current transients, as shown in Fig. 5 (right). It is worth noting that the application of an inappropriate voltage vector following a wrong current prediction has limited effects on the current transient, both in time and amplitude. Actually, the RLS algorithm modifies the covariance matrix to correct the prediction. The availability in few control periods T_c of a reliable prediction assures quite limited effects on the controlled current at startup. Anyway, the amplitude on the current transients is strictly related to the ratio between the bus voltage and the inductances of the motor, as inferable from (4). The higher the ratio, the smaller the control period required to get satisfactory performances.

As a general remark, large inductances are quite normal in synchronous motors with dominant reluctance torque component as in the present case. Nevertheless, there can be a large variability in the inductance value for other motor topologies. As one can observe from (11), the updating of the covariance matrix $\mathbf{Q}(k)$ is influenced only by the regressor vector $\mathbf{\Phi}$ and the forgetting factor f and not by motor parameters. After few control periods one can assume that the prediction algorithm works correctly. The dynamics of the current control are still influenced by the motor inductances, but their values are not relevant for a successful motor startup.

B. Tuning of the forgetting factor

The only parameter that has to be tuned in the proposed scheme is the forgetting factor f in (11). The PMAREL motor is dragged at its nominal speed Ω_N by the load motor. The switch SW in Fig. 3 is in the state 1. Three current steps, each with a different value of forgetting factor f, are performed on the d-axis. The results are reported in Fig. 6a. Similar results can be obtained on the q-axis.

The coefficients evolution during the current steps are reported in Fig. 6b, Fig. 6c and Fig. 6d. The coefficients values were normalised with respect to the nominal current I_N. It is worth noting that in Fig. 6 the coefficients do not start from zero since the recording started when the motor was already in the steady state condition. For the sake of showing the complete transient of the coefficients, a longer time window was used compared to the one in Fig. 6a.

The forgetting factor value influences directly the promptness of the coefficients $\mathbf{p}_d$ and $\mathbf{p}_q$ estimation. It can be noticed from in Fig. 6b that the higher the value of f, the slower the estimation of $p_{2,d}$. This is an intrinsic feature of the RLS algorithm in (11): a value of f close to one means that the oldest measurements are equally weighted to estimate the actual value of the coefficients. On the contrary, smaller values of f force the RLS algorithm to consider only the latest measurements, but increasing the value of the covariance $\mathbf{Q}$ as inferable from (11).

The delay in the case of $f = 0.98$ does not affect significantly the d-axis current dynamics reported in 6a. This is due to the fact that the differential inductance l_d does not change considerably during the current step (see (4)).

An interesting result of the test in Fig. 6 is obtained by observing $\widehat{p}_{1,q}$ in Fig. 6d. Before the current step, i.e. at zero dq-axes currents, $p_{1,d}$ is null, while $p_{1,q}$ is not null. This is due to the back-electromotive force induced by the permanent magnets as inferable from (8), since $\lambda_d(0, 0) = \Lambda_{\text{pm}}$ as highlighted in Fig. 4. As a final remark, the data collected during the current step have shown that the current prediction error is not significantly affected by the choice of the forgetting factor, at least within the normal range adopted in RLS algorithms.

C. Influence of speed on $\widehat{\mathbf{p}}_d$ and $\widehat{\mathbf{p}}_q$ estimation

It is worth recalling that parameters $p_{1,q}$ and $p_{1,d}$ are also strongly influenced by the operating speed as inferable from (3) and (8), respectively. The PMAREL motor speed is controlled by means of a PI speed regulator, which corresponds to the switch position $SW = 2$ in Fig. 3.

A speed ramp transient is commanded at no load condition from zero till the nominal speed. The results are reported in Fig. 7. The d-axis coefficient $p_{1,d}$ increases linearly with the speed because of the motional term in (3). The coefficient $p_{1,q}$ increases as well, but with a rather different slope. It is quite straight from (8) that the current variation δi_q^0 value depends on the differential inductance l_q and the d-axis flux λ_d. However, l_q is considerably higher than l_d and thus the slope of the current variation is smaller. A higher slope of the coefficient $p_{1,q}$ is obtained by increasing the permanent magnet flux linkage, such as the case of interior permanent magnet motors. The experiment has also revealed that a speed variation increases the noise of the current prediction error, but the compensation given by (18) assures that the error remains within a range of $\pm 1\%$ of the rated current.

D. Influence of current on $\widehat{\mathbf{p}}_d$ and $\widehat{\mathbf{p}}_q$ estimation

In order to show the load influence on the coefficients $\widehat{\mathbf{p}}_d$ and $\widehat{\mathbf{p}}_q$ estimation, a q-axis current ramp test was carried out. The result is reported in Fig. 8. The speed was maintained by the load motor, and the motor under test was control in torque mode by selecting $SW = 1$ in Fig. 3.

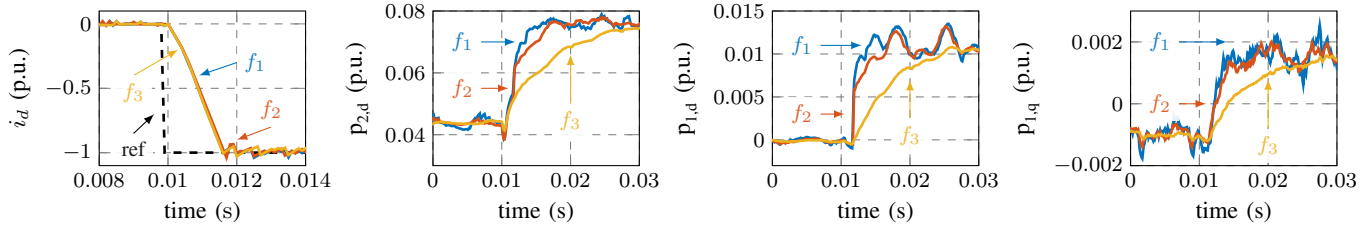

(a) Current measurements (b) Estimated δi_d^f amplitude (c) Estimated δi_d^0 amplitude (d) Estimated δi_q^0 amplitude

Fig. 6. Tuning of the forgetting factor f: d-axis current step with $f_1 = 0.9$, $f_2 = 0.94$, $f_3 = 0.98$.

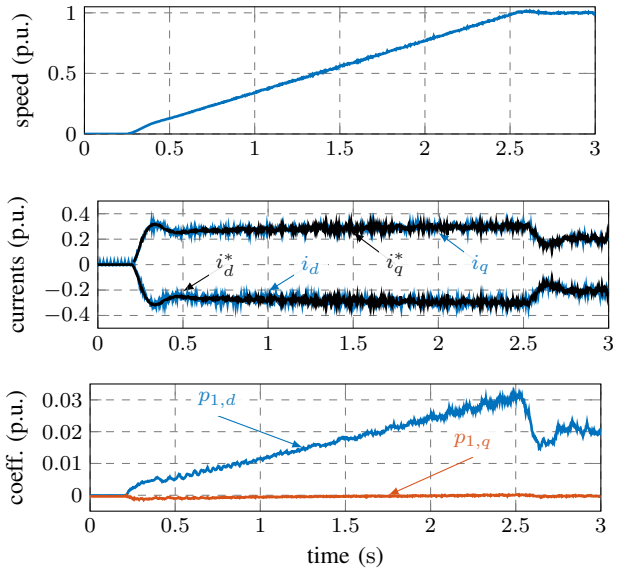

Fig. 7. Estimation of $p_{1,d}$ and $p_{1,q}$ during a speed ramp.

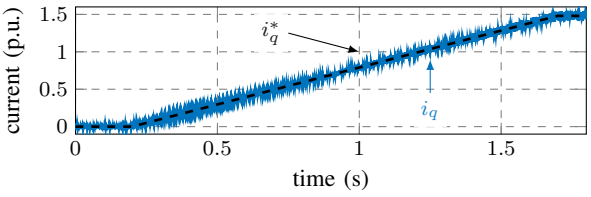

(a) q-current tracking

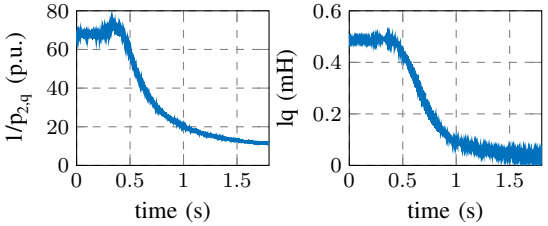

(b) Estimated δi_q^f amplitude (c) q-axis differential inductance

Fig. 8. Estimation of δi_q^f amplitude during a q current ramp: $\Omega = \Omega_N$, $i_d^* = 0\,p.u.$.

The coefficient $\widehat{p}_{2,q}$ estimation is reported in Fig. 8b and it allows to draw interesting considerations. Its value changes with the current, that is the terms in (9) are changing with the load. Therefore, the value of $\widehat{p}_{2,q}$ is strongly related to the value of the differential inductance l_q. A visual comparison between the coefficient $\widehat{p}_{2,q}$ and the parameter l_q in Fig. 8b and 8c, respectively, confirms this relationship.

In case of unknown motor applied to the drive, it is possible to find out a magnetic anisotropy by simply observing the values of $\widehat{p}_{2,d}$ and $\widehat{p}_{2,q}$. Different magnetic characteristics imply different inductances and thus different coefficients. This feature of the proposed algorithm goes toward the evolution of plug-and-play drives at which this paper aims.

The experiment led also to the conclusion that the current prediction errors remain negligible because the RLS algorithm is able to track efficiently the variation of the differential inductance due to the moving working point (see Fig. 8).

E. Comparison between predictive control algorithms

For the sake of generality, the proposed algorithm is compared with other two different predictive control algorithms. It was recently proposed a new control paradigm including the *model-free* concept [19]–[22]. The technique proposed in this paper is inherently close to the model-free paradigm and the comparison between them is proposed. In particular, the technique proposed in [21] was used as term of comparison. Furthermore, the results of the same tests obtained with a model-based MPC controller are reported, too. Differential inductances and motor fluxes are not constant in the model, such as in (2), as proved by the magnetic fluxes curves in Fig. 4. The implemented model-based MPC featured an interpolation algorithm to obtain the correct magnetic fluxes based on the dq-axes currents. The stator resistance variation is neglected in the implementation.

A load step test was carried out at different speeds. The motor under test was controlled in speed control mode, i.e. $SW = 2$ in Fig. 3. The load reference is thus set by the PI speed regulator and the current references are obtained by means of the MTPA curve. Two different speed values were considered aiming at showing the performances of the proposed algorithm along the whole nominal speed range of the motor under test.

A high speed test was carried out by maintaining the nominal speed. The nominal load was applied step like and the results of speed and currents measurements are reported

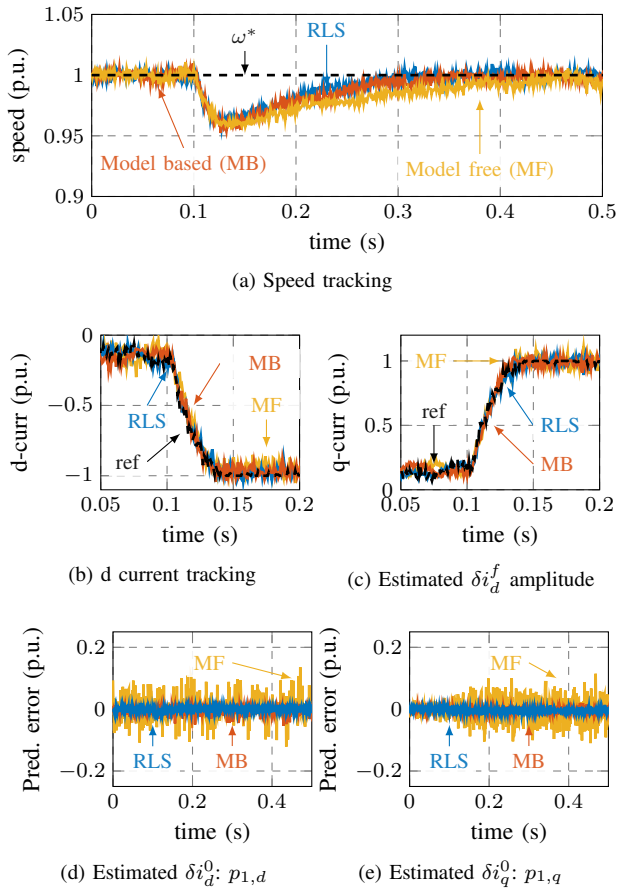

(a) Speed tracking

(b) d current tracking

(c) Estimated δi_d^f amplitude

(d) Estimated δi_d^0: $p_{1,d}$

(e) Estimated δi_q^0: $p_{1,q}$

Fig. 9. Comparison between finite-set current controllers at the nominal point.

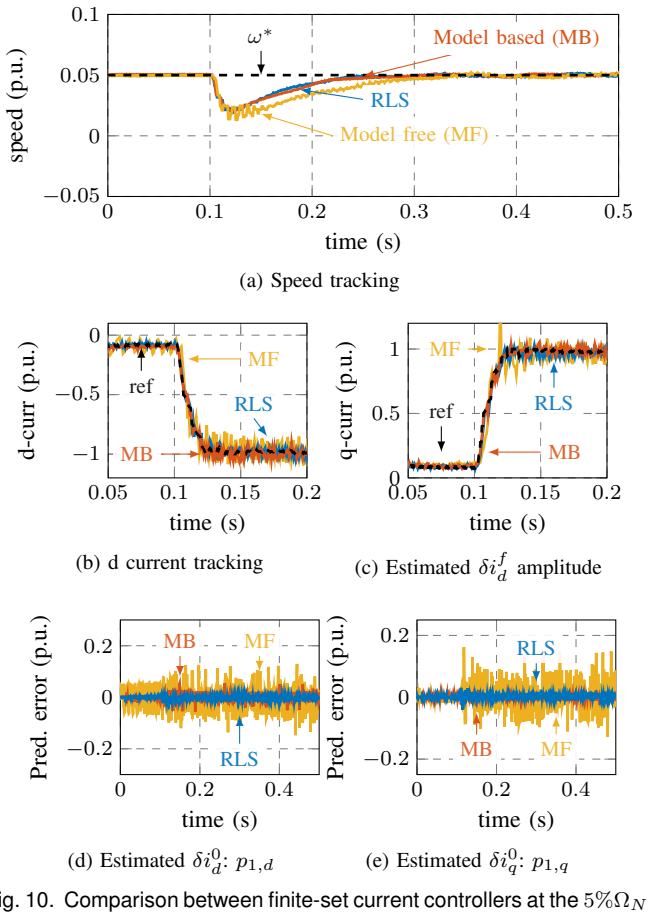

(a) Speed tracking

(b) d current tracking

(c) Estimated δi_d^f amplitude

(d) Estimated δi_d^0: $p_{1,d}$

(e) Estimated δi_q^0: $p_{1,q}$

Fig. 10. Comparison between finite-set current controllers at the $5\%\Omega_N$.

in Fig. 9a and 9b, respectively. It is known from literature [21] that the model-free solution reduces its performances for increasing speed and load. The prediction error is calculated by the difference between the predicted and measured currents and the results are reported in Fig. 9d and Fig. 9e for d- and q-axes, respectively. The improvements in the current prediction of the proposed technique respect to the model-free ones are quite relevant. Finally, the prediction errors of the proposed algorithm are comparable with the ones obtained by the model-based MPC solution. The results are surprisingly quite similar, even though the latter solution remains slightly superior.

Comparable results are obtained also at low speed (Fig. 10), where the model-free solution of [21] is less affected by the speed-dependent terms, but it is still dependent on the load. The prediction error results of Fig. 10d and 10e confirms the better accuracy of the proposed solution. Furthermore, the results of the proposed solution are very close to the model-based MPC ones.

In general, the proposed solution allows to sensibly improve the performances of the model-free solution. This is due to the filtering effect of the RLS algorithm in (11) which permits a rather better current variation estimation. Under the light of the results in Fig. 9 and 10, it is reasonable to say that a more sophisticated estimation scheme, such as the RLS, justifies the efforts of constructing a proper model of the system under consideration. The key-point of the proposed technique is to consider only the current variations and describe them by means of an equivalent model using a description similar to the free and forced response of the motor currents.

V. Conclusion

An adaptive finite-set MPC current regulator has been proposed in this paper. No information about motor electric parameters are required to control the synchronous motor under test. The necessary information are obtained by means of two recursive least square estimators, one for each axis.

The coefficients extrapolated using the recursive least square algorithms are exploited in the prediction phase of the MPC controller. Several tests are reported in order to highlight the relationships between motor working conditions and estimated parameters, in particular the influence of the working speed and currents. The effects of the forgetting factor in the recursive least square estimators are also discussed by means of experiment.

The results of the proposed method improve sensibly the performances of the model-free predictive control algorithm presented in the scientific literature. Interesting benefits are achieved in terms of prediction error and current tracking performances. The price to pay is a more sophisticated solution, which still does not require any information about the motor parameters.

As a result of the proposed technique, future drives could move towards a plug-and-play configuration. The results of the

technique proposed in this paper show that the current tracking performances are not significantly compromised. One of the main advantages of the proposed technique is that complicated self-commissioning procedures for parameter estimation may be avoided, at least initially.

REFERENCES

[1] S. Vazquez, J. Rodriguez, M. Rivera, L. G. Franquelo, and M. Norambuena, "Model predictive control for power converters and drives: Advances and trends," *IEEE Trans. Ind. Electron.*, vol. 64, no. 2, pp. 935–947, Feb 2017.

[2] J. Rodriguez, M. P. Kazmierkowski, J. R. Espinoza, P. Zanchetta, H. Abu-Rub, H. A. Young, and C. A. Rojas, "State of the art of finite control set model predictive control in power electronics," *IEEE Trans. Ind. Informat.*, vol. 9, no. 2, pp. 1003–1016, May 2013.

[3] L. Guo, N. Jin, C. Gan, L. Xu, and Q. Wang, "An improved model predictive control strategy to reduce common-mode voltage for two-level voltage source inverters considering dead-time effects," *IEEE Trans. Ind. Electron.*, vol. 66, no. 5, pp. 3561–3572, May 2019.

[4] J. Liu, C. Gong, Z. Han, and H. Yu, "IPMSM model predictive control in flux-weakening operation using an improved algorithm," *IEEE Trans. Ind. Electron.*, vol. 65, no. 12, pp. 9378–9387, Dec 2018.

[5] J. Falck, G. Buticchi, and M. Liserre, "Thermal stress based model predictive control of electric drives," *IEEE Trans. Ind. Appl.*, vol. 54, no. 2, pp. 1513–1522, March 2018.

[6] Y. Luo and C. Liu, "A simplified model predictive control for a dual three-phase PMSM with reduced harmonic currents," *IEEE Trans. Ind. Electron.*, vol. 65, no. 11, pp. 9079–9089, Nov 2018.

[7] A. Favato, P. G. Carlet, F. Toso, and S. Bolognani, "A model predictive control for synchronous motor drive with integral action," in *IECON 2018 - 44th Annual Conference of the IEEE Industrial Electronics Society*, Oct 2018, pp. 325–330.

[8] X. Zhang, L. Zhang, and Y. Zhang, "Model predictive current control for pmsm drives with parameter robustness improvement," *IEEE Trans. Power Electron.*, vol. 34, no. 2, pp. 1645–1657, Feb 2019.

[9] R. Antonello, L. Ortombina, F. Tinazzi, and M. Zigliotto, "Online stator resistance tracking for reluctance and interior permanent magnet synchronous motors," *IEEE Trans. Ind. Appl.*, vol. 54, no. 4, pp. 3405–3414, July 2018.

[10] K. Liu, Q. Zhang, J. Chen, Z. Q. Zhu, and J. Zhang, "Online multiparameter estimation of nonsalient-pole PM synchronous machines with temperature variation tracking," *IEEE Trans. Ind. Electron.*, vol. 58, no. 5, pp. 1776–1788, May 2011.

[11] L. Peretti, P. Sandulescu, and G. Zanuso, "Self-commissioning of flux linkage curves of synchronous reluctance machines in quasi-standstill condition," *IET Electric Power Appl.*, vol. 9, no. 9, pp. 642–651, 2015.

[12] N. Bedetti, S. Calligaro, and R. Petrella, "Stand-still self-identification of flux characteristics for synchronous reluctance machines using novel saturation approximating function and multiple linear regression," *IEEE Trans. Ind. Appl.*, vol. 52, no. 4, pp. 3083–3092, July 2016.

[13] S. A. Odhano, P. Pescetto, H. A. A. Awan, M. Hinkkanen, G. Pellegrino, and R. Bojoi, "Parameter identification and self-commissioning in AC motor drives: A technology status review," *IEEE Trans. Power Electron.*, vol. 34, no. 4, pp. 3603–3614, April 2019.

[14] M. Pulvirenti, G. Scarcella, G. Scelba, A. Testa, and M. M. Harbaugh, "On-line stator resistance and permanent magnet flux linkage identification on open-end winding PMSM drives," *IEEE Trans. Ind. Appl.*, vol. 55, no. 1, pp. 504–515, Jan 2019.

[15] S. Nalakath, M. Preindl, and A. Emadi, "Online multi-parameter estimation of interior permanent magnet motor drives with finite control set model predictive control," *IET Electric Power Applications*, vol. 11, no. 5, pp. 944–951, 2017.

[16] W. Deng, C. Xia, Y. Yan, Q. Geng, and T. Shi, "Online multiparameter identification of surface-mounted PMSM considering inverter disturbance voltage," *IEEE Trans. Energy Convers.*, vol. 32, no. 1, pp. 202–212, March 2017.

[17] C. Zhang, G. Wu, F. Rong, J. Feng, L. Jia, J. He, and S. Huang, "Robust fault-tolerant predictive current control for permanent magnet synchronous motors considering demagnetization fault," *IEEE Trans. Ind. Electron.*, vol. 65, no. 7, pp. 5324–5334, July 2018.

[18] Z. Chen, J. Qiu, and M. Jin, "Adaptive finite-control-set model predictive current control for IPMSM drives with inductance variation," *IET Electric Power Appl.*, vol. 11, no. 5, pp. 874–884, 2017.

[19] C. Lin, T. Liu, J. Yu, L. Fu, and C. Hsiao, "Model-free predictive current control for interior permanent-magnet synchronous motor drives based on current difference detection technique," *IEEE Trans. Ind. Electron.*, vol. 61, no. 2, pp. 667–681, Feb 2014.

[20] C. Lin, J. Yu, Y. Lai, and H. Yu, "Improved model-free predictive current control for synchronous reluctance motor drives," *IEEE Trans. Ind. Electron.*, vol. 63, no. 6, pp. 3942–3953, June 2016.

[21] S. Bolognani, P. G. Carlet, F. Tinazzi, and M. Zigliotto, "Fast and robust model free predictive current control for synREL motor drives," in *2018 IEEE ECCE*, Sep. 2018, pp. 5466–5472.

[22] P. G. Carlet, F. Tinazzi, S. Bolognani, and M. Zigliotto, "An effective model-free predictive current control for synchronous reluctance motor drives," *IEEE Trans. Ind. Appl.*, pp. 1–1, 2019.

[23] T. Söderström and P. Stoica, *System Identification*, 1st ed. Prentice Hall International, 1989.

Fabio Tinazzi (M'16) received the B.S. and M.S., Ph.D. degree in Mechatronic Engineering from University of Padova in 2008, 2011 and 2015 respectively. Since February 2017, he is a Researcher at the Department of Management and Engineering, University of Padova, Vicenza, Italy. His main research interests include sensorless control, predictive control and parameter estimation techniques for ac motors.

Paolo Gherardo Carlet Paolo Gherardo Carlet received the B.S. and M.S. degree (hons.) in electrical engineering in 2015 and 2017, respectively, from the University of Padova, Padova, Italy. He is currently working toward the Ph.D. degree with the Electrical Drives Laboratory, University of Padova. His main interests include sensorless and predictive control for ac motor drives.

Silverio Bolognani (M'98, SM'16, F'2019) received the Laurea degree in Electrical Engineering from the University of Padova, Italy, in 1976. He is author of more than 250 publications about design and control of electrical drives. He was Head of the Department of Electrical Engineering from 2001 to 2008, and vice-Rector for the Research from 2009 to 2015 at the Padova University. He is currently a Full Professor of Electrical Converters, Machines and Drives.

Mauro Zigliotto (M'98, SM'18) received the Laurea degree in Electronic Engineering from the University of Padova, Padua, Italy, in 1988. He is full professor of Electrical Machines and Drives at University of Padova, Italy and head of the Electric Drives Laboratory in Vicenza, Italy. Advanced control strategies and self-commissioning for ac motors are Prof. Zigliotto's main research interests.